analytical chemistry

pubs.acs.org/ac Article

One-Step Surface Modification to Graft DNA Codes on Paper: The Method, Mechanism, and Its Application

Wan Zhou, Mengli Feng, Alejandra Valadez, and XiuJun Li*

Cite This: *Anal. Chem.* 2020, 92, 7045−7053 Read Online

ACCESS | Metrics & More | Article Recommendations | Supporting Information

ABSTRACT: Glass slides have been widely used for DNA immobilization in DNA microarray and numerous bioassays for decades, whereas they are faced with limitations of low probe density, time-consuming modification steps, and expensive instruments. In this work, a simple one-step surface modification method using 3-aminopropyl trimethoxysilane (APTMS) has been developed and applied to graft DNA codes on paper. Higher DNA immobilization efficiency was obtained in comparison with that in a conventional method using glass slides. Fluorescence detection, X-ray photoelectron spectroscopy (XPS), infrared spectra (FT-IR), and pH influence studies were employed to characterize the surface modification and subsequent DNA immobilization, which further reveals a mechanism in which this method lies in ionic interactions between the positively charged APTMS-modified paper surface and negatively charged DNA probes. Furthermore, an APTMS-modified paper-based device has been developed to demonstrate application in low-cost detection of a foodborne pathogen, *Giardia lamblia*, with high sensitivity (the detection limit of 22 nM) and high specificity. Compared with conventional methods using redundant cross-linking reactions, our method is simpler, faster, versatile, and lower-cost, enabling broad applications of paper-based bioassays especially for point-of-care detection in resource-poor settings.

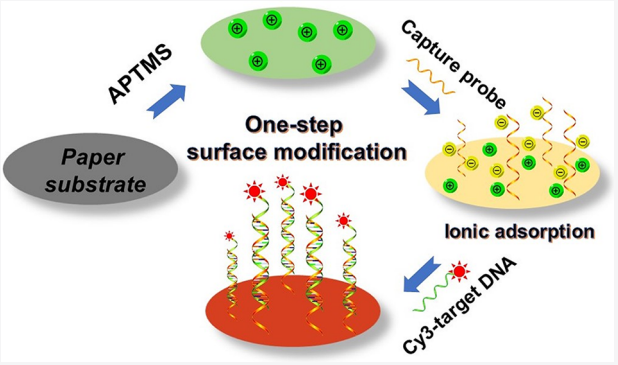

Over past decades, DNA microarray technology that is generally accomplished via covalent or noncovalent immobilization of DNA capture probes on certain substrates has been widely used in various biological applications.[1] Among these substrates, glass slides are most commonly used for biomolecular detection in microarray technologies, mainly due to excellent optical properties and minimal compatibility issues with most organic solvents.[2,3] Moreover, multiple conventional surface modification methods have been developed to construct microarrays, which primarily rely on the reaction of piranha solution-treated glass surfaces with alkoxysilane-appended aldehydes, carboxylic acids, or amines.[3−5] Despite these advances, traditional glass slide substrates suffer from inherent difficulties, such as complicated surface modification processes, low probe density, high cost, the need for expensive and bulky equipment, and prolonged detection times.[6,7] Therefore, there have been increasing demands for a capable, robust, and affordable substrate that comes with facile DNA probe immobilization for genetic applications.

Paper, a widely available cellulosic material, is composed of a large matrix of cellulose fibers with a three-dimensional (3D) porous structure.[8,9] Paper materials have many advantages including low production cost, high porosity, high portability and durability, and a high degree of availability in our daily life.[10,11] Thus, paper becomes an excellent candidate of substrate for many applications. A growing number of emerging applications for paper materials are currently being explored and developed to bind, activate, isolate, and detect different molecules for different applications because of the ease of manipulation and low costs associated with paper-based materials,[12] such as environmental studies, water and food safety monitoring, and point-of-care (POC) diagnostics.[13−23] To achieve those applications, different strategies have been employed for biomolecule immobilization onto cellulosic paper.[24−30] For example, divinyl sulfone (DVS) and 1,4-phenylenediisothiocyanate (PDITC) were used by Yu et al. and Araujo et al., respectively, for the covalent attachment of oligonucleotides onto cellulose membranes.[24,25] Moreover, among various functionalities used for immobilization on the paper surface, the *N*-hydroxysuccinimide (NHS) ester group has been most widely used for DNA probe immobilization due

Received: January 21, 2020
Accepted: March 24, 2020
Published: March 24, 2020

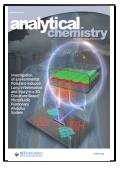

https://dx.doi.org/10.1021/acs.analchem.0c00317
Anal. Chem. 2020, 92, 7045−7053

to its specific reaction with amine or hydrazide functional groups.[26,27] Although the aforementioned covalent biomolecular immobilization strategies have been successfully employed in various biological applications, most of them require multistep surface modification processes including redundant cross-linking reactions and further modification of DNA probes with corresponding functional groups such as $-NH_2$, preventing their wide applications.[31]

To address these challenges, we have developed a simple, one-step, versatile, and low-cost surface modification method to graft DNA codes onto cellulose paper. In this novel strategy, the cellulose paper was simply modified with 3-aminopropyl trimethoxysilane (APTMS) and then directly applied to immobilize nonfunctionalized DNA probes. Different DNA immobilization experiments were performed on two substrates (cellulose paper and glass slides) using different immobilization methods (i.e., our method and a conventional covalent bonding method) to test and compare the DNA immobilization performance. In addition, fluorescence microscopy, X-ray photoelectron spectroscopy (XPS), and Fourier transform infrared spectroscopy (FT-IR) were utilized to characterize the surface modification and the subsequent DNA immobilization. It is worth noting that our exploration further revealed the mechanism of the proposed DNA immobilization method, which lies in ionic interaction between the positively charged paper surface and negatively charged DNA probes. The influence of pH on DNA immobilization was further studied systematically to verify the aforementioned mechanism. Furthermore, after the optimization of incubation conditions, this modification method was successfully applied to develop a low-cost paper-based device for the pathogen detection of *Giardia lamblia*, with a limit of detection (LOD) of 22 nM. Compared with conventional methods, this method is simpler, faster, and lower-cost, which will become a valuable asset and provide an accessible "universal" tool for numerous nucleic acids-related applications, especially for POC detection in low-resource settings.

Scheme 1 illustrates the main principle of our one-step surface modification method. Our method is very simple, and it only requires one-step modification by a common reagent, APTMS. As shown in Scheme 1A, the original cellulose paper is filled with many hydroxyl groups (−OH). In our method, APTMS is simply applied on cellulose paper under ambient conditions to introduce amine groups on the paper surface, which involves a condensation reaction between APTMS and existing −OH groups on the paper surface. Then, the paper becomes ready to graft DNA probes. In the new strategy, we hypothesize that the surface of the APTMS-modified paper that is covered with amino groups ($-NH_2$) could be effectively positively charged under certain conditions, mainly due to protonated cations ($R-NH_3^+$) in a pH range lower than its pK_a. On the other hand, it is known that DNA molecules are negatively charged due to their backbone phosphate groups.[32] Hence, negatively charged single-strand DNA (ssDNA) probes can be easily immobilized on the paper surface due to electrostatic attraction between these oppositely charged ions, as shown in Scheme 1A. It is worthwhile to mention that, although we use $-NH_2$ terminated ssDNA in the scheme (mainly for the convenience in the comparison with a conventional DNA immobilization method subsequently), our method actually does not require any functionalization of ssDNA, which significantly decreases the cost and the complexity of the assay and meanwhile increases the universality of ssDNA and the assay.[33] As a comparison, Scheme 1B illustrates a conventional surface modification process to covalently immobilize DNA onto the paper surface, in which paper is first modified using APTMS and followed by cross-linking reactions with terephthalic acid (TA).[34,35] After the surface modification, $-NH_2$ functionalization and additional EDC (1-ethyl-3[dimethylaminopropyl] carbodiimide hydrochloride)/Sulfo-NHS (*N*-hydroxysulfosuccinimide) cross-linking steps are required for the ssDNA to be immobilized on paper. Additionally, to compare the immobilization efficiency of cellulosic paper and glass slides, similar experiments were also performed on glass slides to covalently immobilize DNA following a modified reported procedure in Scheme S1.[36] Compared to the newly proposed method, the conventional APTMS/TA cross-linking method requires multiple steps; several cross-linking reagents including TA, EDC, and Sulfo-NHS; extra functionalization of ssDNA; and prolonged time. The detailed information regarding cross-linking reactions (as illustrated in Scheme S2) can be found in the Supporting Information.

Scheme 1. Schematic Illustration of the One-Step Surface Modification Method for DNA Immobilization on Cellulose Paper vs a Conventional Method Based on Terephthalic Acid Cross-Linking Reaction[a]

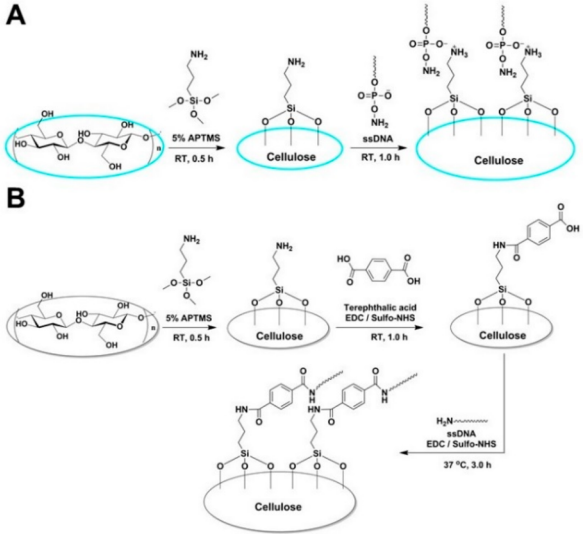

[a](A) The ssDNA immobilization onto the APTMS-modified paper via a direct, one-step ionic adsorption. (B) The ssDNA immobilization onto the multistep surface-modified paper via terephthalic acid cross-linking reactions.

EXPERIMENT SECTION

Reagents and Materials. Whatman no. 1 chromatography paper (20 × 20 cm), (3-aminopropyl) trimethoxysilane (97%, APTMS), fluorescein isothiocyanate (FITC), bovine serum albumin (BSA), terephthalic acid (TA), sodium hydroxide (NaOH), hydrogen peroxide (H_2O_2), and phosphate buffer saline (PBS) were purchased from Sigma-Aldrich (St. Louis, MO). 1-Ethyl-3[dimethylaminopropyl] carbodiimide hydrochloride (EDC·HCl) was purchased from Advanced ChemTech (Louisville, KY). *N*-hydroxysulfosuccinimide (Sulfo-NHS) was purchased from Thermo Scientific (Rockford, IL). Sulfuric acid was purchased from Alfa Aesar (Ward Hill, MA). SU-8 (2010) was purchased from Microchem (Newton,

https://dx.doi.org/10.1021/acs.analchem.0c00317
Anal. Chem. 2020, 92, 7045−7053

MA). Plain glass microscope slides (75 mm × 25 mm.) were purchased from Fisher Scientific (Hampton, NH). Polydimethylsiloxane (PDMS, Sylgard 184) was obtained from Dow Corning (Midland, MI). Washing buffer (2× SSC/0.1% SDS) was freshly prepared from 20× SSC buffer (Sigma-Aldrich (St. Louis, MO)). Ultrapure Milli-Q water (18.2 MΩ·cm) was obtained from a Millipore water purification system (Bedford, MA). Unless otherwise stated, all chemicals were of analytical grade and used as received. All oligonucleotides were synthesized and modified by Integrated DNA Technologies (Coralville, IA), with all ssDNA sequences listed in Table S1.

One-Step Surface Modification of the Patterned Paper. The patterned paper was fabricated (see details in the Supporting Information) and placed on an orbital shaker after plasma treatment for 4 min and then treated with 5% APTMS in 95% ethanol for 30 min under ambient temperature. The patterned paper was then rinsed three times with 95% ethanol and deionized water, respectively, to remove excess reagents and then dried in the air. The APTMS-modified paper was stored in the dark at 4 °C prior to the probe immobilization.

Grafting DNA Codes on the APTMS-Modified Paper. Two microliters of 1 μM Cy3-labeled ssDNA per detection zone was added onto the APTMS-modified cellulose paper and followed by incubation for 1 h at room temperature. The cellulose paper was then rinsed with washing buffer and dried under ambient temperature. Fluorescence images were captured after each washing step via Nikon Ti-E fluorescence microscopy (Melville, NY) with an exposure time of 9 ms, and the fluorescence intensities were analyzed using the Nikon Element software. The fluorescence excitation wavelength was 550 nm, and the excitation wavelength was 568 nm. All other experimental details are included in the Supporting Information.

RESULTS AND DISCUSSION

Surface Characterization of the APTMS-Modified Paper with Fluorescence Microscopy. To confirm the successful surface modification by APTMS in our one-step method, comparison experiments between modified and native paper were conducted by exploiting the reaction between the amine-terminated paper surface and fluorescein isothiocyanate (FITC, Figure 1), a widely used fluorescent probe to label primary amino groups. The reaction mechanism is illustrated in Figure 1A. In short, FITC was added to the unmodified paper as well as the APTMS-modified paper and followed by washing three times. Fluorescence signals were detected on a Nikon Ti-E fluorescence microscope and are shown in Figure 1B. It can be seen that strong fluorescence signals were observed on the APTMS-modified paper, while no fluorescence was observed on the unmodified paper. The fluorescence intensity increased by ~30 fold from 246 a.u. using unmodified paper to 7493 a.u. using APTMS-modified paper, which confirmed successful surface modification on cellulose paper with APTMS. These results can be attributed to a condensation reaction between primary amines on APTMS-modified paper and thiocyanates,[37] yielding thioureas and the introduction of fluorophores onto the paper surface. This APTMS-modified/isothiocyanate reaction resulted in strong fluorescence signals in the detection zones. In contrast, when applied to unmodified paper, FITC was easily carried away by washing buffer and resulted in no fluorescence, since no chemical reaction occurred between FITC and the unmodified paper surface.

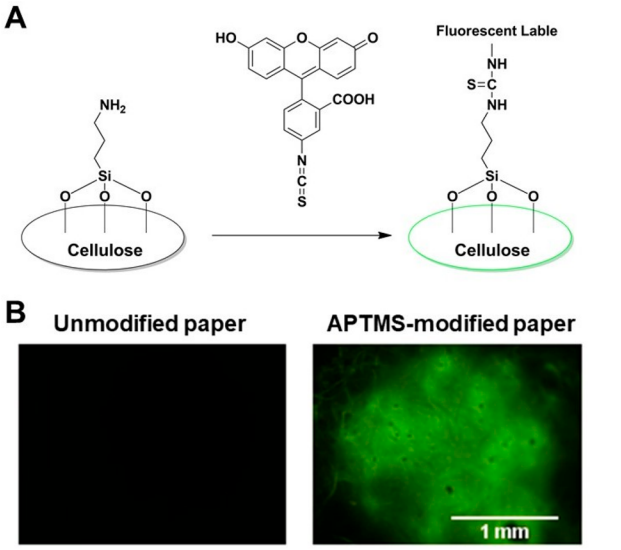

Figure 1. Surface characterization of APTMS-modified paper with fluorescence microscopy. (A) Reaction scheme between FITC and the APTMS-modified paper. (B) Fluorescence images of the APTMS-modified paper upon the addition of FITC (B, right), using the unmodified paper as a negative control (B, left) after three washes. The concentration of FITC was 0.05 mg/mL. The fluorescence intensity of FITC was obtained at an emission wavelength of 525 nm under an excitation at 488 nm.

XPS Characterization of the Surface Modification and DNA Immobilization on the APTMS-Modified Paper. To further verify the surface modification and subsequent DNA functionalization of cellulose paper, XPS surface analysis was performed. On the basis of XPS elemental compositional results (Table 1, see also the Supporting Information, Figure S1), only carbon (C 1s peak centered at ~284.6 eV) and oxygen (O 1s peak centered at ~531.0 eV) signals were detected at the surface of unmodified cellulose paper, which agreed well with the composition of cellulosic paper, $(C_6H_{10}O_5)_n$.[38−40] After surface modification with APTMS, the appearance of a nitrogen signal, a N 1s peak centered at 399.0 eV, with an atomic percentage estimated to be ~4.4%, revealed that APTMS modified the cellulose paper surface and a certain amount of amino groups were introduced via the silane coupling technique. Moreover, the XPS analysis of ssDNA-functionalized APTMS-modified paper disclosed the immobilization of ssDNA on the modified paper surface, leading to an increase of the atomic percentage of N from 4.4% to 7.5%. The ratio of N/C was found to increase substantially from 6.6% to 11.6%, which explicitly indicated the attachment of ssDNA onto the APTMS-modified paper due to its nitrogen-containing nucleobases. In addition, the ratio of O/

Table 1. XPS Compositional Analysis of Different Paper Substrates

XPS analysis, atomic percentage	unmodified paper	APTMS-modified paper	ssDNA-functionalized paper
C 1s	71.4%	66.5%	64.6%
O 1s	28.6%	29.2%	27.3%
N 1s		4.4%	7.5%

https://dx.doi.org/10.1021/acs.analchem.0c00317
Anal. Chem. 2020, 92, 7045−7053

C remained similar for the above samples, implying that the basic elemental composition of paper substrates did not change much during surface modification and DNA immobilization procedures.

FT-IR Characterization of the Surface Modification and DNA Immobilization on the APTMS-Modified Paper. To identify silicon- and nitrogen-containing bonding on paper substrates and gain insight into the ionic adsorption mechanism, the paper surface was further characterized by FT-IR (Spectrum 100 FT-IR Spectrometer, PerkinElmer, UK). The FT-IR spectra of the unmodified paper, the APTMS-modified paper, and the DNA-functionalized APTMS-modified paper were recorded and shown in Figure 2. Specifically, the

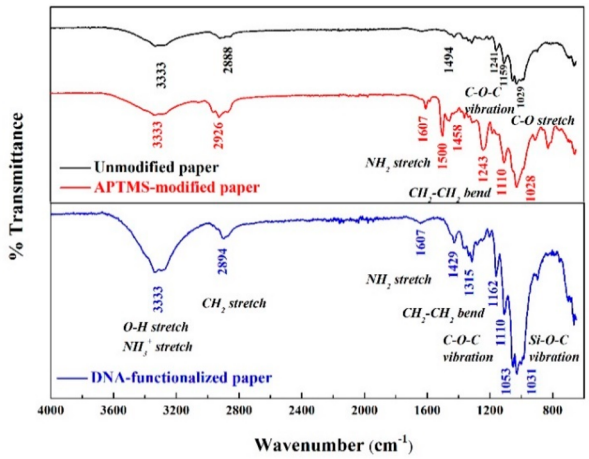

Figure 2. FT-IR spectra characterization of unmodified paper (black), APTMS-modified paper (red), and DNA-functionalized paper (blue). ssDNA without $-NH_2$ functionalization was used herein.

FT-IR spectra in Figure 2 (black) demonstrated typical peaks of cellulose paper: O−H stretching vibration region from ca. 3200 to 3500 cm^{-1}, C−O−C asymmetric vibration from ca. 1162 to 1125 cm^{-1}, and C−O stretching vibration region from ca. 1030 to 1060 cm^{-1}.[41−43] In the case of the APTMS-modified paper, as shown in Figure 2 (red), the absorption peaks around ca. 1030 cm^{-1}, ca. 1607 cm^{-1}, and ca. 2900 cm^{-1} were ascribed to the Si−O−C bond, $-NH_2$ bending, and CH_2 stretching vibration, respectively, which indicated the existence of aminopropyl silane groups.[42] In addition, the bending vibration of methylene groups was observed in the region from ca. 1420 to 1500 cm^{-1}. As for the ssDNA-functionalized APTMS-modified paper, in which ssDNA without $-NH_2$ functionalization was used for the immobilization, Figure 2 (blue) shows that the absorption bands of $-NH_3^+$ and −OH stretching vibrations appeared from ca. 3280 to 3380 cm^{-1}, while the $-NH_2$ bending vibration at ca. 1607 cm^{-1} became weaker, which could be assigned to the transformation from $-NH_2$ to $-NH_3^+$.[44] Moreover, vibration peaks from ca. 1110 to 1500 cm^{-1}, which were attributed to C−O bonds and methylene bending vibrations,[43] became markedly weaker in comparison with those in the APTMS-modified paper as expected. This phenomenon and the appearance of $-NH_3^+$ absorption bands agreed well with our hypothesis that DNA codes would be grafted onto the APTMS-modified paper mainly due to ionic interactions between the positively charged paper surface and negatively charged DNA molecules, which weakened the above vibrations.[45]

Studies of pH Influence on DNA Immobilization on the APTMS-Modified Paper and the Ionic Adsorption Mechanism. According to the proposed mechanism, pH can affect the charges on $-NH_2$ groups on the APTMS-modified paper surface and thus plays a significant role in the DNA immobilization process on the APTMS-modified paper. To further confirm that DNA immobilization goes through the ionic interaction mechanism, the pH influence on the grafting of DNA codes onto APTMS-modified paper was investigated by studying different DNA immobilization efficiencies under different pH conditions, based on the distinct molecular charge distribution of amine groups on the paper surface and phosphate groups on DNA molecules in different pH media. Since pH is an important variable affecting DNA immobilization,[5,46] this study can also provide optimal conditions for efficient DNA immobilization on paper. Cy3-labeled DNA with different pH values from pH 1.0 to 14.0 was added on the APTMS-modified paper followed by washing three times. The corresponding fluorescence intensities (from Cy3) were recorded separately by the fluorescence microscopy. Results from Figure 3A show fluorescence intensities increased steadily

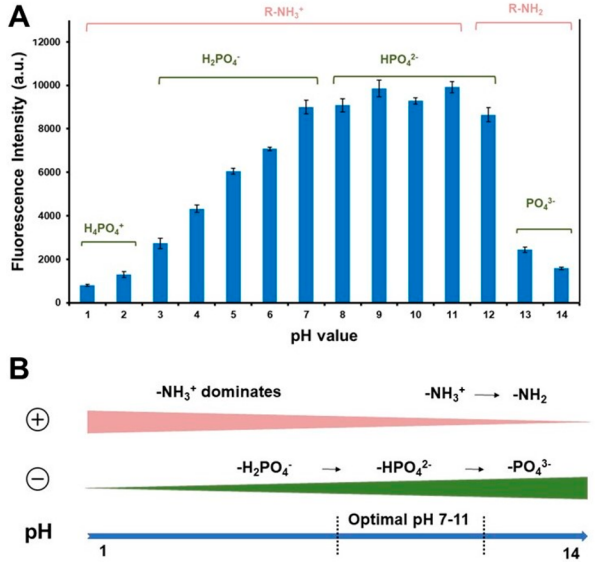

Figure 3. PH influence studies confirming a mechanism of ionic interaction between DNA molecules and the APTMS-modified paper. (A) Fluorescence intensities of Cy3-labeled DNA on APTMS-modified paper vs different pH values from 1.0 to 14.0. Different species dominate interactions between the APTMS-modified surface and phosphate groups of DNA probes while pH varies. Error bars represent standard deviations (n = 6). (B) Schematic of charge changes and main species of APTMS-modified paper surface and DNA molecules while pH varies. Positively charged ions on paper dominate the reaction at lower pH (<7.0), while negatively charged DNA molecules dominate the reaction at high pH (>11.0). The optimal pH range for DNA immobilization on APTMS-modified paper is 7.0−11.0.

from pH 1.0 to pH 7.0, plateaued from pH 7.0 to 12.0, and then decreased distinctly when pH was above 12.0. The results are the consequence of the mutual interaction between factors under varying conditions: positively charged ions ($R-NH_3^+$ when pH < 11.0) on the paper surface and negative charges on DNA molecules with different pK_a values. As illustrated in Figure 3B, at low pH (pH < 11.0), the protonated cations ($R-NH_3^+$) are predominant on the APTMS-modified paper

https://dx.doi.org/10.1021/acs.analchem.0c00317
Anal. Chem. 2020, 92, 7045−7053

surface, since the pK_a of APTMS−NH_3^+ is 11.0.[47,48] Therefore, the paper surface is positively charged when pH was lower than 11.0 or so and becomes less and even not positively charged at higher pH. In other words, the higher the pH, the worse the DNA immobilization from the paper surface side. Hence, pH values higher than 11.0 are not beneficial for the DNA immobilization due to minimal positive charges (see the trend of positive charge changes from Figure 3B, pink). That is why the DNA immobilization efficiency was a minimum at pH values of 13.0−14.0, no matter how many negative charges from the DNA side. On the other hand, as reported previously, the three pK_a values of phosphoric acid are 2.1, 7.2, and 12.5, respectively.[49−51] The amount of negative charges on DNA molecules increases as pH increases, because different species ($H_2PO_4^-$, HPO_4^{2-}, and PO_4^{3-}) become dominant with increasing pH values (Figure 3B). In other words, the higher the pH, the better the DNA immobilization for the DNA side (see the trend of negative charge changes from Figure 3B, green). Hence, pH values lower than 2.1 are not beneficial to the DNA immobilization due to minimal negative charges from the DNA side. That is why the DNA immobilization efficiency was a minimum at pH values of 1.0−2.0. The combined net effects from both the DNA side and the APTMS-modified paper surface side actually impact the final DNA immobilization, especially in the pH range of 3.0 to 12.0. From pH 3.0 to 7.0, the increase of negative charges from the DNA side dominates and is the limiting factor of the DNA immobilization performance (while the positive charges from the paper side are saturated), leading to gradual increases of fluorescence intensities. Similarly, from pH 11.0 to 13.0, the decrease of positive charges from the APTMS-modified paper side dominates and is the limiting factor of the DNA immobilization performance (while the negative charges from the paper side are saturated), resulting in dramatic decreases of fluorescence intensities. The middle pH range from 7.0 to 11.0 included factors beneficial to the DNA immobilization from both sides, enabling the highest DNA performance in this pH range. Therefore, the optimal pH range for grating DNA codes on APTMS-modified paper was determined to be 7.0−11.0. More importantly, this pH influence study confirmed the proposed mechanism: the DNA immobilization on the APTMS-modified surface goes through an ionic adsorption mechanism.

Comparison of DNA Immobilization Efficiency on the APTMS-Modified Paper vs Glass Substrates and Conventional Surface Modification Methods. To demonstrate high efficiency of DNA immobilization by the proposed strategy, we performed DNA immobilization on different substrates using different methods with Cy3-labeled ssDNA, including the APTMS-modified paper (APTMS-paper), the terephthalic acid-modified paper (TA-paper), and the terephthalic acid-modified glass slides (TA-glass). Fluorescence signals were recorded using fluorescence microscopy, and the results are summarized in Figure 4 (see also the Supporting Information, Figure S2). According to the images prior to washing (Figure 4A), stronger fluorescence signals appeared on cellulosic paper substrates than those on glass slides. After washing, the fluorescence signals on both APTMS-paper and TA-paper remained superior, while a significant loss of fluorescence signals was found on TA-glass. It suggested that paper substrates were advantageous over glass slides to graft DNA molecules, which was attributed to the 3D porous structure of paper substrates. Figure 4B shows the fluorescence

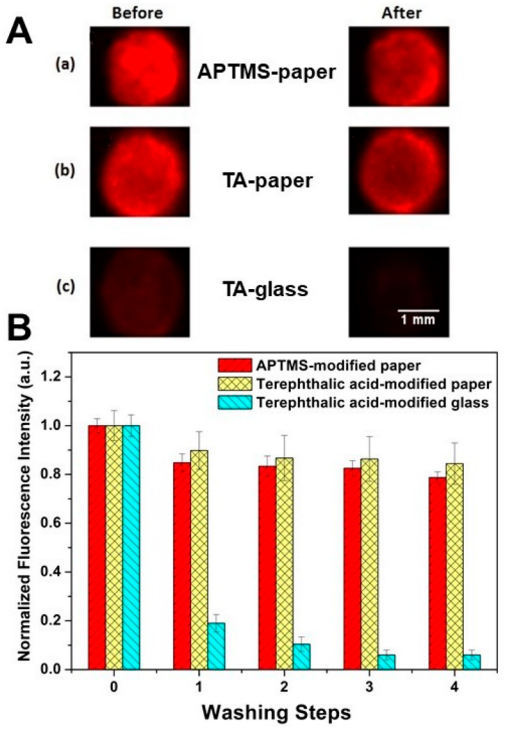

Figure 4. Fluorescence characterization of DNA immobilization on different substrates. (A) Fluorescence images on different substrates: (a) ATPMS-modified paper (APTMS-paper), (b) terephthalic acid-modified paper (TA-paper), and (c) terephthalic acid-modified glass slides (TA-glass) before and after four washing steps. (B) Fluorescence signals vs washing steps on different substrates: APTMS-modified paper (red), terephthalic acid-modified paper (yellow), and terephthalic acid-modified glass slides (aqua). Error bars represent standard deviations (n = 6).

changes with different washing steps. It can be seen that with the increase of washing steps, there was only a slight decrease (less than 20%) of normalized fluorescence intensities on both APTMS-modified paper and TA-modified paper, whereas an obvious decrease (more than 80%) of fluorescence signals was exhibited on TA-modified glass slides only after the first washing step. This dramatic decrease (down to 6.0% after four washes) indicated the low density of immobilized DNA molecules on glass slides. In contrast, after multiple washing processes, the APTMS-modified paper exhibited much higher DNA immobilization levels (80%) than that on glass. Although the TA-modified paper exhibited a slightly higher DNA immobilization level (84%) than the APTMS-modified paper, it required multiple complicated steps for the paper surface modification and DNA immobilization. Additionally, fluorescence signals on the unmodified paper were recorded and compared with APTMS-modified paper, TA-modified paper, and TA-modified glass after the fourth washing step (Figure S2). It was found that after washing steps, DNA molecules were washed away from unmodified paper, whereas the fluorescence intensity on the APTMS-modified paper substrate was nearly 40 times higher than that of the unmodified paper after the fourth washing step. The comparison between our method and the conventional method in Table 2 lists more details, including procedures, functionalization of ssDNA, time, material cost, and so on. Taking all the above results together, we can conclude that our proposed one-step method has provided high efficiency for simple DNA immobilization on

https://dx.doi.org/10.1021/acs.analchem.0c00317
Anal. Chem. 2020, 92, 7045−7053

Table 2. Comparison Between the Proposed Paper Surface Modification Method Using APTMS and the Conventional Glass Surface Modification Method Using TA

substrate	surface modification	modification reagents	surface modification time	functionalization of ssDNA	DNA immobilization method	material cost ($)[a]
cellulose paper	one step	APTMS	0.5 h	no need	ionic adsorption	~0.06
glass slides	multistep	TA, EDC, Sulfo-NHS	>3.0 h	$-NH_2$	cross-linking reactions	~18.00

[a]The material cost is calculated based on both substrates (cellulose paper or glass slides) and major modification reagents (APTMS, TA, EDC, and Sulfo-NHS) per detection.

paper without cumbersome and time-consuming covalent modification steps.

Condition Optimization of Grafting DNA Codes on the APTMS-Modified Paper. To demonstrate biological applications of this new method, experimental conditions such as the incubation temperature and incubation time were first optimized. The incubation temperature during ssDNA immobilization, as an important factor in DNA detection, would affect the efficiency of DNA immobilization as well as fluorescent signals. Incubation assays at different typical temperatures as previously reported,[52,53] such as 4 °C (in the fridge), 25 °C (room temperature), 37 °C, and 42 °C, were investigated, and the results are shown in Figure 5A. The incubation at 42 °C gave the highest fluorescence signals compared to the rest. Hence, 42 °C was used in the following DNA detection. Additionally, the incubation time would also affect the immobilization efficiency of DNA on paper. Herein, a series of incubation times of 1 h, 2 h, 3 h, and overnight (~12 h) were selected, and the immobilization performance was studied in this context. It was found that fluorescence signals were similar under the above incubation times, as shown in Figure 5B. Therefore, 1 h of incubation time was deemed enough for the DNA immobilization and was selected as the standard incubation time in the subsequent experiments.

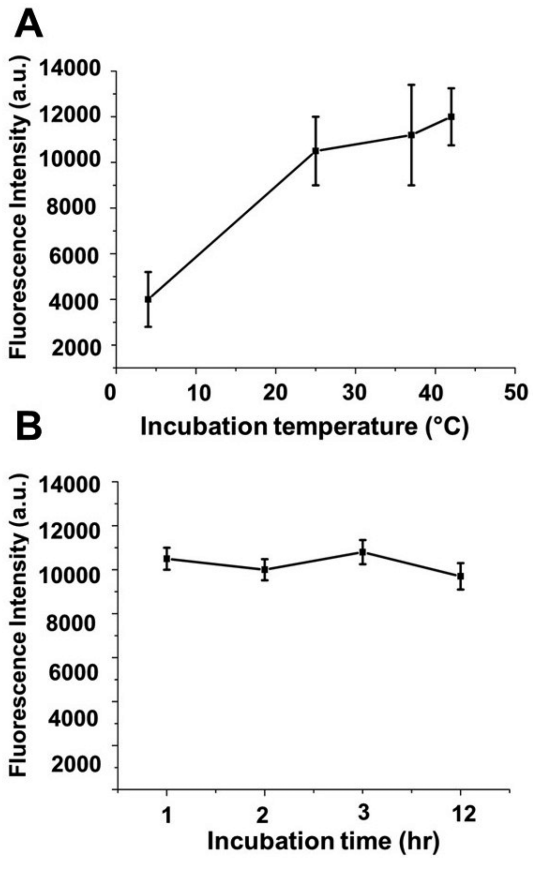

Figure 5. Condition optimization of DNA immobilization on the APTMS-modified paper. (A) Fluorescence intensities of Cy3-labeled DNA immobilized on the APTMS-modified paper under different incubation temperatures (4 °C, 25 °C, 37 °C, and 42 °C). (B) Fluorescence intensities of Cy3-labeled DNA immobilized on APTMS-modified paper under different incubation times (1, 2, 3, and 12 h). Error bars represent standard deviations (n = 6).

Biological Application of Grafting DNA Codes on the APTMS-Modified Paper. Using optimized conditions, we have developed a low-cost paper-based device via DNA testing to demonstrate a diagnostic application for the rapid detection of a foodborne pathogen, *Giardia lamblia*. *Giardia lamblia*, also known as *Giardia intestinalis* and *Giardia duodenalis*, is one of the most pathogenic intestinal parasites of mammals and humans worldwide.[54,55] It commonly causes diarrheal illness throughout the world, especially in developing countries, resulting from water-borne and food-borne infections. Detection of *Giardia lamblia* DNA is critical to better understanding and identifying different genotypes and is crucial to diagnoses and treatments of the disease.[56] In this work, *Giardia lamblia* DNA was used as a model pathogen to develop a bioassay on a paper-based device. As illustrated in Figure 6A, the paper-based device with 6 × 5 hydrophilic zones surrounded by hydrophobic barriers was fabricated using the photolithography method (see the Supporting Information).[57,58] The hydrophilic zones were treated with our one-step surface modification method using APTMS, generating adequate positive charges on paper surface. Then, negatively charged DNA capture probes were immobilized onto the hydrophilic zones via simple ionic adsorption (Figure 6A), followed by DNA hybridization with the pathogen target, *Giardia* DNA. In this diagnostic test, Cy3-labeled *Giardia* amplicon and *N. Meningitis* amplicon were used as the positive control (PC) and the negative control (NC), respectively, while the PBS buffer was used as the background. Fluorescence signals were collected from each detection zone. As the *Giardia* DNA concentration increased in the range from 10 to 1000 nM, as shown in Figure 6B, the fluorescence intensity was proportional to the sample concentration, with a square of the correlation coefficient of 0.98. There was no significant change in fluorescence intensities when increasing the concentration of the negative control and the PBS buffer. The LOD of Cy3-*Giardia* DNA was calculated based on a 3-fold standard deviation above the blank and determined as low as 22 nM, which is comparable to that in refs 4, 59, and 60 or even about 30-fold lower than those reported on glass slides (e.g., 0.6 μM).[61]

CONCLUSION

In summary, a facile one-step surface modification method has been developed for grafting DNA codes on a low-cost porous

https://dx.doi.org/10.1021/acs.analchem.0c00317
Anal. Chem. 2020, 92, 7045−7053

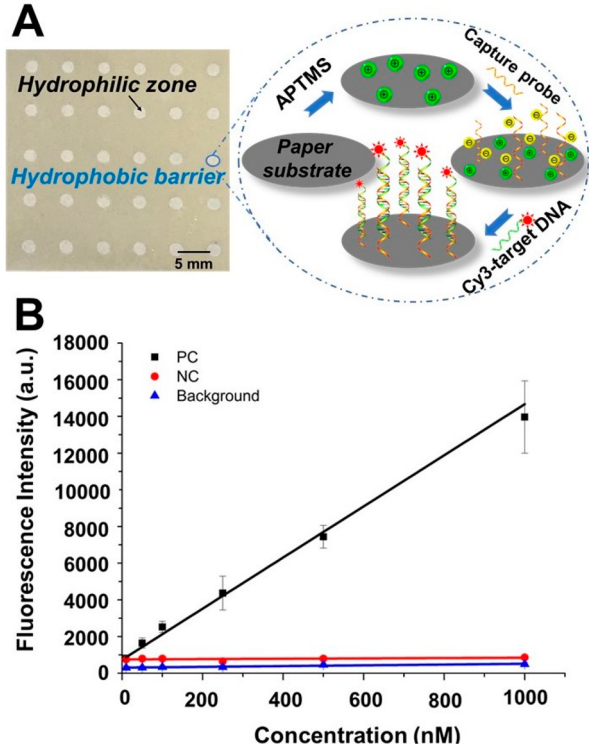

Figure 6. Diagnostic application of the one-step surface modification method for *Giardia lamblia* DNA detection on a paper-based device. (A) Image of a patterned paper-based device using the photolithography method. The inset is the schematic illustration of the diagnostic assay on the device, including the paper surface modification process using APTMS, capture DNA probes immobilization on paper, and DNA hybridization process. (B) Calibration curve of *Giardia lamblia* detection via DNA hybridization on the APTMS-modified paper-based device, with positive controls (black), negative controls (red), and the PBS buffer as a background (blue). Error bars represent standard deviations (n = 6).

material, paper. Fluorescence characterization, XPS, and FT-IR spectra and a pH effect study confirmed successful surface modification and DNA immobilization and verified the proposed mechanism of ionic adsorption between DNA molecules and APTMS-modified paper. We also developed a paper-based device based on the one-step surface modification method and applied it to the low-cost detection of the foodborne pathogen *Giardia lamblia*. The calibration curve was obtained with high detection sensitivity (the detection limit of 22 nM) in a wide dynamic range from 10 nM to 1000 nM.

Compared to the conventional glass surface modification method for DNA immobilization, the proposed method is advantageous in many aspects, as listed in Table 2. First, it is simple, and only a one-step procedure is needed to modify the paper surface instead of multistep procedures for glass surface modification. Additionally, DNA immobilization does not require EDC/Sulfo-NHS cross-linking steps, significantly reducing the complexity of DNA assays. Second, the one-step procedures for the surface modification and the DNA immobilization significantly decrease the needed time from >3.0 to 0.5 h. Third, there is no need of any functionalization of DNA probes in the immobilization process, leading to a universal strategy for all types of DNA testing. Fourth, when taking into account the different substrates (cellulose paper and glass slides) and major surface modification reagents (APTMS, TA, EDC, and Sulfo-NHS) used in the two methods, APTMS-modified paper yields a 300-fold decrease in cost for each assay compared to TA-modified glass. Finally, thanks to the high porosity of paper, our one-step method can enhance DNA immobilization efficiency and detection sensitivity. Although fluorescence detection was used herein to demonstrate the application for simple DNA immobilization on paper, this one-step surface modification method can be further applied in other biomolecular detection methods, such as the widely used colorimetric detection on paper-based devices, simply by changing fluorescent probes to colorimetric DNA probes or aptamers. Given extensive research in DNA probes- or DNA aptamers-related colorimetric detection using paper-based devices (e.g., lateral flow assays), we envisage this method can also be applied to numerous colorimetric biomolecular analyses on paper-based devices, especially for the POC testing. Overall, this facile one-step method for surface modification and DNA immobilization on paper has great potential for numerous genetic assays and applications, particularly in resource-poor settings. The low-cost porous material, paper, may emerge as a new promising substrate for a wide range of genetic analysis and other biomolecular applications.[62−64]

■ ASSOCIATED CONTENT

Supporting Information

The Supporting Information is available free of charge at https://pubs.acs.org/doi/10.1021/acs.analchem.0c00317.

Additional experimental details and results on DNA sequences, the fabrication of paper-based devices, surface modification process, DNA immobilization process and schemes, XPS, and fluorescence detection data (PDF)

■ AUTHOR INFORMATION

Corresponding Author

XiuJun Li − *Department of Chemistry and Biochemistry, Biomedical Engineering, Border Biomedical Research Center, and Environmental Science and Engineering, The University of Texas at El Paso, El Paso, Texas 79968, United States;* orcid.org/0000-0002-7954-0717; Email: xli4@utep.edu

Authors

Wan Zhou − *Department of Chemistry and Biochemistry, The University of Texas at El Paso, El Paso, Texas 79968, United States;* orcid.org/0000-0002-1439-9548

Mengli Feng − *Department of Chemistry and Biochemistry, The University of Texas at El Paso, El Paso, Texas 79968, United States*

Alejandra Valadez − *Department of Chemistry and Biochemistry, The University of Texas at El Paso, El Paso, Texas 79968, United States*

Complete contact information is available at: https://pubs.acs.org/10.1021/acs.analchem.0c00317

Notes

The authors declare the following competing financial interest(s): The authors X.L. and W.Z. submitted a U.S. patent (pending) and have financial interest in the work. The other authors have no financial interest in the work.

https://dx.doi.org/10.1021/acs.analchem.0c00317
Anal. Chem. 2020, 92, 7045−7053

■ ACKNOWLEDGMENTS

We are grateful for the financial support to the work from the National Institute of General Medical Sciences of the NIH (SC2GM105584), the U.S. NSF PREM Program (DMR 1827745), the Emily Koenig Meningitis Fund and Philadelphia Foundation, and the Medical Center of the Americas Foundation. Financial support from NSF I-Corps (IIP 1953841), NIH/NIAID (R21AI107415), the NIH RCMI Pilot Grant, the NIH BUILDing Scholar Summer Sabbatical Award, the University of Texas at El Paso for the IDR Program, and the University of Texas System for the STARS Award is also gratefully acknowledged. We also thank Prof. Siddhartha Das for kindly providing *Giardia lamblia* DNA samples, and the Dr. Keelung Hong Research Fellowship for the fellowship to W.Z.

■ REFERENCES

(1) Pirrung, M. C. *Angew. Chem., Int. Ed.* **2002**, *41* (8), 1276−1289.
(2) Lee, M. R.; Shin, I. *Angew. Chem., Int. Ed.* **2005**, *44* (19), 2881−2884.
(3) Lee, K.; Rouillard, J. M.; Pham, T.; Gulari, E.; Kim, J. *Angew. Chem., Int. Ed.* **2007**, *46* (25), 4667−4670.
(4) Schlapak, R.; Pammer, P.; Armitage, D.; Zhu, R.; Hinterdorfer, P.; Vaupel, M.; Frühwirth, T.; Howorka, S. *Langmuir* **2006**, *22* (1), 277−285.
(5) Ham, H. O.; Liu, Z.; Lau, K.; Lee, H.; Messersmith, P. B. *Angew. Chem.* **2011**, *123* (3), 758−762.
(6) Wang, L.; Li, P. C. *J. Agric. Food Chem.* **2007**, *55* (26), 10509−10516.
(7) Sanjay, S. T.; Dou, M.; Sun, J.; Li, X. *Sci. Rep.* **2016**, *6*, 30474.
(8) Zang, D.; Ge, L.; Yan, M.; Song, X.; Yu, J. *Chem. Commun.* **2012**, *48* (39), 4683−4685.
(9) Martinez, A. W.; Phillips, S. T.; Whitesides, G. M.; Carrilho, E. *Anal. Chem.* **2010**, *82* (1), 3−10.
(10) Martinez, A. W.; Phillips, S. T.; Butte, M. J.; Whitesides, G. M. *Angew. Chem., Int. Ed.* **2007**, *46* (8), 1318−1320.
(11) Lu, Y.; Shi, W.; Jiang, L.; Qin, J.; Lin, B. *Electrophoresis* **2009**, *30* (9), 1497−1500.
(12) Cate, D. M.; Adkins, J. A.; Mettakoonpitak, J.; Henry, C. S. *Anal. Chem.* **2015**, *87* (1), 19−41.
(13) Ellerbee, A. K.; Phillips, S. T.; Siegel, A. C.; Mirica, K. A.; Martinez, A. W.; Striehl, P.; Jain, N.; Prentiss, M.; Whitesides, G. M. *Anal. Chem.* **2009**, *81* (20), 8447−8452.
(14) Jokerst, J. C.; Adkins, J. A.; Bisha, B.; Mentele, M. M.; Goodridge, L. D.; Henry, C. S. *Anal. Chem.* **2012**, *84* (6), 2900−2907.
(15) Dou, M. W.; Dominguez, D. C.; Li, X. J.; Sanchez, J.; Scott, G. *Anal. Chem.* **2014**, *86* (15), 7978−7986.
(16) Dou, M.; Sanjay, S. T.; Dominguez, D. C.; Liu, P.; Xu, F.; Li, X. *Biosens. Bioelectron.* **2017**, *87*, 865−873.
(17) Dou, M. W.; Sanjay, S. T.; Benhabib, M.; Xu, F.; Li, X. J. *Talanta* **2015**, *145*, 43−54.
(18) Tang, R. H.; Liu, L. N.; Zhang, S. F.; He, X. C.; Li, X. J.; Xu, F.; Ni, Y. H.; Li, F. *Microchim. Acta* **2019**, *186* (8), 521.
(19) Dou, M.; Macias, N.; Shen, F.; Dien Bard, J.; Dominguez, D. C.; Li, X. *EClinicalMedicine* **2019**, *8*, 72−77.
(20) Xu, X. Y.; Wang, X. M.; Hu, J.; Gong, Y.; Wang, L.; Zhou, W.; Li, X. J.; Xu, F. *Electrophoresis* **2018**, *40* (6), 914−921.
(21) Dou, M.; Sanchez, J.; Tavakoli, H.; Gonzalez, J. E.; Sun, J.; Dien Bard, J.; Li, X. *Anal. Chim. Acta* **2019**, *1065*, 71−78.
(22) Tavakoli, H.; Zhou, W.; Ma, L.; Guo, Q.; Li, X. *Paper and Paper Hybrid Microfluidic Devices for Point-of-Care Detection of Infectious Diseases*; Wiley-VCH: Nanotechnology and Microfluidics, 2020; pp 177−209.
(23) Jin, Q.; Ma, L.; Zhou, W.; Shen, Y.; Fernandez-Delgado, O.; Li, X. J. *Chem. Sci.* **2020**, *11*, 2915.
(24) Yang, J.-H.; Song, K.-S.; Zhang, G.-J.; Degawa, M.; Sasaki, Y.; Ohdomari, I.; Kawarada, H. *Langmuir* **2006**, *22* (26), 11245−11250.
(25) Araújo, A. C.; Song, Y.; Lundeberg, J.; Ståhl, P. L.; Brumer, H., III *Anal. Chem.* **2012**, *84* (7), 3311−3317.
(26) Wu, Y.; Xue, P.; Hui, K. M.; Kang, Y. *Biosens. Bioelectron.* **2014**, *52*, 180−187.
(27) Zhu, Y.; Xu, X.; Brault, N. D.; Keefe, A. J.; Han, X.; Deng, Y.; Xu, J.; Yu, Q.; Jiang, S. *Anal. Chem.* **2014**, *86* (6), 2871−2875.
(28) Scida, K.; Li, B. L.; Ellington, A. D.; Crooks, R. M. *Anal. Chem.* **2013**, *85* (20), 9713−9720.
(29) Teengam, P.; Siangproh, W.; Tuantranont, A.; Vilaivan, T.; Chailapakul, O.; Henry, C. S. *Anal. Chem.* **2017**, *89* (10), 5428−5435.
(30) Prasad, K. S.; Cao, X. Y.; Gao, N.; Jin, Q. J.; Sanjay, S. T.; Henao-Pabon, G.; Li, X. J. *Sens. Actuators, B* **2020**, *305*, 127516.
(31) Yu, A.; Shang, J.; Cheng, F.; Paik, B. A.; Kaplan, J. M.; Andrade, R. B.; Ratner, D. M. *Langmuir* **2012**, *28* (30), 11265−11273.
(32) Thorsness, P. E.; Koshland, D. E. *J. Biol. Chem.* **1987**, *262* (22), 10422−10425.
(33) Zhou, W.; Hu, K. Q.; Kwee, S.; Tang, L.; Wang, Z. H.; Xia, J. F.; Li, X. J. *Anal. Chem.* **2020**, *92* (3), 2739−2747.
(34) Moon, R. J.; Martini, A.; Nairn, J.; Simonsen, J.; Youngblood, J. *Chem. Soc. Rev.* **2011**, *40* (7), 3941−3994.
(35) Park, S.; Pai, J.; Han, E. H.; Jun, C. H.; Shin, I. *Bioconjugate Chem.* **2010**, *21* (7), 1246−1253.
(36) Wang, H.; Li, J.; Liu, H.; Liu, Q.; Mei, Q.; Wang, Y.; Zhu, J.; He, N.; Lu, Z. *Nucleic Acids Res.* **2002**, *30* (12), 61e.
(37) Guan, L.; Tian, J.; Cao, R.; Li, M.; Wu, Z.; Nilghaz, A.; Shen, W. *BioResources* **2014**, *10* (1), 1587−1598.
(38) He, Q.; Ma, C.; Hu, X.; Chen, H. *Anal. Chem.* **2013**, *85* (3), 1327−1331.
(39) Malekghasemi, S.; Kahveci, E.; Duman, M. *Talanta* **2016**, *159*, 401−411.
(40) Zhang, H.; Lee, N. Y. *Appl. Surf. Sci.* **2015**, *327*, 233−240.
(41) Koga, H.; Kitaoka, T.; Isogai, A. *J. Mater. Chem.* **2011**, *21* (25), 9356−9361.
(42) Kao, P.-K.; Hsu, C.-C. *Microfluid. Nanofluid.* **2014**, *16* (5), 811−818.
(43) Zhao, M.; Li, H.; Liu, W.; Guo, Y.; Chu, W. *Biosens. Bioelectron.* **2016**, *79*, 581−588.
(44) Hijazi, M.; Rieu, M.; Stambouli, V.; Tournier, G.; Viricelle, J. P.; Pijolat, C. *Procedia Eng.* **2016**, *168*, 280−283.
(45) Li, X.; Liu, L.; Schlegel, H. B. *J. Am. Chem. Soc.* **2002**, *124* (32), 9639−9647.
(46) Zhang, X.; Servos, M. R.; Liu, J. *J. Am. Chem. Soc.* **2012**, *134* (17), 7266−9.
(47) Wang, X.; Niu, D.; Li, P.; Wu, Q.; Bo, X.; Liu, B.; Bao, S.; Su, T.; Xu, H.; Wang, Q. *ACS Nano* **2015**, *9* (6), 5646−5656.
(48) Shalev, G.; Cohen, A.; Doron, A.; Machauf, A.; Horesh, M.; Virobnik, U.; Ullien, D.; Levy, I. *Sensors* **2009**, *9* (6), 4366−4379.
(49) Christ, P.; Lindsay, A. G.; Vormittag, S. S.; Neudörfl, J. M.; Berkessel, A.; O'Donoghue, A. C. *Chem. - Eur. J.* **2011**, *17* (31), 8524−8528.
(50) Birlik Demirel, G. *ChemPhysChem* **2014**, *15* (8), 1693−1699.
(51) Wang, J.; Bard, A. J. *Anal. Chem.* **2001**, *73* (10), 2207−2212.
(52) Josephson, L.; Perez, J. M.; Weissleder, R. *Angew. Chem.* **2001**, *113* (17), 3304−3306.
(53) Kam, N. W. S.; Liu, Z.; Dai, H. *Angew. Chem.* **2006**, *118* (4), 591−595.
(54) Adam, R. D. *Clin. Microbiol. Rev.* **2001**, *14* (3), 447−475.
(55) Schulz, D.; Holstein, J. M.; Rentmeister, A. *Angew. Chem., Int. Ed.* **2013**, *52* (30), 7874−7878.
(56) Mero, S.; Kirveskari, J.; Antikainen, J.; Ursing, J.; Rombo, L.; Kofoed, P. E.; Kantele, A. *Infect. Dis.* **2017**, *49* (9), 655−663.
(57) Tavakoli, H.; Zhou, W.; Ma, L.; Perez, S.; Ibarra, A.; Xu, F.; Zhan, S. H.; Li, X. J. *TrAC, Trends Anal. Chem.* **2019**, *117*, 13−26.
(58) Sanjay, S. T.; Zhou, W.; Dou, M. W.; Tavakoli, H.; Ma, L.; Xu, F.; Li, X. J. *Adv. Drug Delivery Rev.* **2018**, *128*, 3−28.
(59) Pirri, G.; Damin, F.; Chiari, M.; Bontempi, E.; Depero, L. E. *Anal. Chem.* **2004**, *76* (5), 1352−1358.

https://dx.doi.org/10.1021/acs.analchem.0c00317
Anal. Chem. 2020, 92, 7045−7053

(60) Le Berre, V.; Trévisiol, E.; Dagkessamanskaia, A.; Sokol, S.; Caminade, A. M.; Majoral, J. P.; Meunier, B.; François, J. *Nucleic Acids Res.* **2003**, *31* (16), e88.
(61) Berdat, D.; Marin, A.; Herrera, F.; Gijs, M. A. M. *Sens. Actuators, B* **2006**, *118* (1−2), 53−59.
(62) Li, Z. D.; You, M. L.; Bai, Y. M.; Gong, Y.; Xu, F. *Small Methods* **2019**, 1900459.
(63) Li, F.; You, M.; Li, S.; Hu, J.; Liu, C.; Gong, Y.; Yang, H.; Xu. *Biotechnol. Adv.* **2020**, *39*, 107442.
(64) You, M.; Li, Z.; Feng, S.; Gao, B.; Yao, C.; Hu, J.; Xu, F. *Trends Biotechnol.* **2020**, DOI: 10.1016/j.tibtech.2019.12.006.

https://dx.doi.org/10.1021/acs.analchem.0c00317
Anal. Chem. 2020, 92, 7045−7053